JOURNAL OF Materials CHEMISTRY

A combined *in situ* X-ray absorption spectroscopy and X-ray diffraction study of the thermal decomposition of ammonium tetrathiotungstate

Richard I. Walton† and Simon J. Hibble*

Department of Chemistry, The University of Reading, Whiteknights, Reading, UK RG6 6AD. E-mail: s.j.hibble@rdg.ac.uk

Received 4th February 1999, Accepted 19th March 1999

The structural changes occurring during the thermal decomposition of ammonium tetrathiotungstate to form amorphous WS_3 and poorly crystalline WS_2 have been studied *in situ* using combined extended X-ray absorption fine structure (EXAFS) spectroscopy at the tungsten L_{III}-edge and X-ray diffraction. Data collected during isothermal decomposition at both 135 and 150 °C show that ammonium tetrathiotungstate decomposes to produce amorphous WS_3 without the formation of any intermediate phases. Decay curves of starting material and growth curves of product derived from both X-ray absorption data and diffraction data show that the two-phase approach to data analysis is appropriate. The fit of various simple kinetic models to the thermal decay curves is tested and it is found that the Prout–Tompkins expression describes the process very well. Heating ammonium tetrathiotungstate from 100 to 350 °C produces first amorphous WS_3 and finally disordered WS_2, a material of catalytic interest. The EXAFS data of this freshly prepared WS_2 are compared to those of crystalline 2H-WS_2. Debye–Waller factors are increased and occupation numbers are significantly reduced from those in the crystalline material for all atomic shells. This behaviour is compared to previous results obtained from poorly crystalline molybdenum disulfide and possible structural models suggested to account for the results of the first EXAFS study of the disordered WS_2.

Introduction

The sulfides of tungsten and molybdenum find practical application in diverse areas. Binary molybdenum sulfides are the active components of industrial hydrodesulfurisation catalysts, used in the purification of petroleum products,[1,2] are used as lubricants both in the solid state and as additives in liquid systems[3] and have been investigated as battery cathode materials for reversible non-aqueous lithium batteries.[4,5] The sulfides of tungsten have also found some use as hydrotreating catalysts.[6] It has been shown that W–Ni hydrodesulfurisation catalysts, which under operating conditions consist of small WS_2 particles, show greater activity and selectivity towards the hydrogenation of aromatic molecules than molybdenum analogues.[7] Recent interest in the tungsten–sulfur system has been aroused by the discovery of tungsten disulfide with inorganic fullerene structures, structural analogues of the now familiar carbon 'bucky balls' and nanotubes; these materials have potential application as solid lubricants.[8,9]

In the past five years, research activity into catalytically active tungsten sulfides has concentrated on the preparation of high surface-area hydrodesulfurisation catalysts by the thermal decomposition of ammonium tetrathiotungstate.[10–13] The materials are poorly crystalline and have composition close to WS_2. A number of workers have independently investigated their properties and have shown that disordered WS_2 exhibits higher catalytic activity towards hydrogenation reactions than transition-metal sulfides prepared by conventional high temperature methods such as the reductive sulfidation of metal oxides.[10–13] Osaki *et al.* attribute the high activity to the small particle size of the WS_2,[10] and other workers have highlighted the low level of oxide impurities in WS_2 prepared by the decomposition routes as being important in explaining the enhanced activity.[12]

It is generally understood that the thermal decomposition of ammonium tetrathiotungstate takes place according to the reaction:

$$(NH_4)_2WS_4 = WS_3 + H_2S\uparrow + 2NH_3\uparrow = WS_2 + S$$

Previous thermogravimetric studies of this process show that when ammonium tetrathiotungstate is heated under an inert atmosphere amorphous tungsten trisulfide (a-WS_3) is produced at temperatures between 170 and 280 °C, and that WS_2 is produced on continued heating between 280 and 330 °C.[14,15] The tungsten disulfide produced by such treatment exists in a poorly crystalline (pc) form and temperatures in excess of 1000 °C are necessary to produce highly crystalline 2H-WS_2. The poorly-ordered material has never been structurally investigated in detail. Two previous groups measured X-ray diffraction patterns of the decomposition products of ammonium tetrathiotungstate at various temperatures and compared them with that of crystalline 2H-WS_2.[14,16] Both studies were performed over 25 years ago and no quantitative information was obtained. Despite the recent interest in the catalytic properties of the material, no further structural investigation has been performed.

Amorphous WS_3, the initial decomposition product of ammonium tetrathiotungstate, is one of a number of amorphous transition-metal chalcogenides that has no crystalline analogue; other examples include MoS_3, Re_2S_7, $MoSe_3$ and WSe_3[17] and the more recently discovered CrS_3, $CrSe_3$, $MoS_{4.7}$, $MoSe_5$, WS_5 and WSe_6.[18,19] These compounds are all more chalcogen-rich than crystalline chalcogenides of each element and their structures have thus attracted considerable attention over the years. The inherent difficulties in the characterisation of structurally disordered materials has meant progress towards the structural description of the amorphous transition-metal chalcogenides has been slow, and in some cases consensus on even a simple structural building block to describe the local environment of constituent atoms has not been reached. Amorphous WS_3 has generally been assumed to be a structural analogue of a-MoS_3, although the structure of the molybdenum sulfide itself is far from being understood, as we have recently discussed.[20,21] Liang and co-workers in the 1980s investigated the amorphous trichal-

†Present address: Inorganic Chemistry Laboratory, South Parks Road, Oxford, UK OX1 3QR.

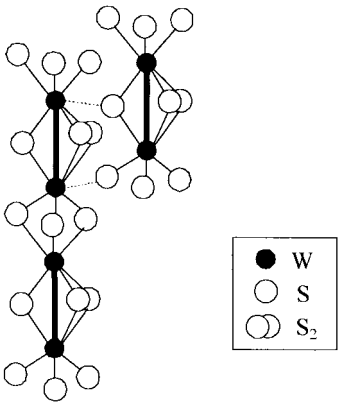

Fig. 1 The widely assumed chain structure of amorphous WS_3. Face-sharing of $\{W^V{}_2S_9\}$ units produces chains with alternating short W–W bonds (*ca.* 2.75 Å indicated by the bold lines), and longer W···W distances. Three of the dimeric units are shown illustrating how short inter-chain W–S interactions may occur (dotted lines).

cogenides of molybdenum and tungsten and concluded that the compounds have chain-like structures with short metal-metal bonds (W–W $\approx$2.75 Å in a-WS_3) by studying radial distribution functions derived from both X-ray diffraction and extended X-ray absorption fine structure (EXAFS) measurements.[22–24] The basis of the chain-model is an M_2S_9 unit (M = Mo, W), in which an M_2 dimer is bridged by monosulfide (S^{2-}) and disulfide ($S_2{}^{2-}$) anions (Fig. 1), and this unit has structural analogues in the extensive coordination chemistry of the group 6 elements with sulfur. The metal may be in oxidation state IV or V, by varying the relative amount of S^{2-} and $(S_2)^{2-}$ ligands per metal atom. The chain structure is formed when the M_2S_9 units are linked by face sharing of the terminal sulfur atoms, and alternating long and short metal–metal interactions are thus expected along a chain. The tungsten–tungsten bonding explains the observed diamagnetism of the compound. Close interchain interactions mean that each tungsten atom may have up to eight near sulfur neighbours (<2.8 Å). In the case of a-MoS_3, an alternative model based on triangular metal–metal bonded Mo_3 clusters has also been postulated on the basis of chemical degradation experiments,[25,26] although our structural investigations suggest that the chain model most accurately describes the structure.[20,21] A similar trinuclear W–W bonded cluster was suggested by Diemann as a structural unit for a-WS_3 in an early study of the structure of the compound.[27] The structure of the compound is clearly far from being fully understood.

Here, we describe the results of an *in situ* study of the thermal decomposition of ammonium tetrathiotungstate using combined EXAFS and powder X-ray diffraction. The method has been shown to be a powerful tool in solid state chemistry, providing a non-invasive means of probing changes in both short- and long-range atomic order during a chemical transformation.[28] It has been applied to a number of systems such as solid-state phase transitions,[28,29] polymerisations,[30] and used widely for the study of solid catalysts under operating conditions.[31,32] We recently described a study of the thermal decomposition of ammonium tetrathiomolybdate using the combined EXAFS/XRD technique, and were able to study for the first time a sample of amorphous MoS_3 freshly prepared *in situ*, and to examine the local order of poorly crystalline MoS_2.[21] On the basis of those results and the current interest in tungsten sulfides we extend our study to the analogous tungsten system.

Experimental

Materials

Ammonium tetrathiotungstate was used as supplied by Aldrich (99.9%). An IR spectrum of the compound showed no characteristic W–O vibrations, indicating that no oxide impurities were present. Crystalline (2H) tungsten disulfide, used as a model compound for the EXAFS experiments, was used as supplied by Aldrich.

The EXAFS/XRD experiment

The combined EXAFS/XRD study was performed on Station 9.3 of the Daresbury SRS using an experimental apparatus previously described by others.[28] The synchrotron source was operating with an average stored-energy of 2 GeV and a typical electron current of 200 mA. EXAFS data were collected at the tungsten L_{III}-edge ($E \approx 10206$ eV) in transmission mode from 13 mm diameter pellets of *ca.* 1 mm thickness of ammonium tetrathiotungstate and crystalline tungsten disulfide finely ground with boron nitride (Alfa). The boron nitride was necessary as a diluent to allow sample concentration to be adjusted to prevent self-absorption ($\mu d \approx 2.5$, $\Delta\mu d \approx 1$), and also acted as a binder to prevent the thin pellets fracturing with the release of the gaseous by-products in the decomposition of ammonium tetrathiotungstate. Boron nitride was suited for these requirements since its powder diffraction pattern exhibits only a small number of well defined Bragg peaks, few of which overlap with those of either ammonium tetrathiotungstate or tungsten disulfide, it undergoes no phase change over the temperature range we studied and it is unreactive towards the materials we investigated. Pellets containing typically 50% by mass of sample were used. EXAFS data were collected in quick-EXAFS mode using a rapidly scanning Si(220) monochromator, with harmonic rejection set at 50% using a mirror situated before the monochromator. The maximum k-value of the data was limited to 16.3 $Å^{-1}$; this data range was sufficient to allow modelling of the parameters describing several atomic shells, but minimised the cycle time of the experiment. The EXAFS data were calibrated using data collected from a tungsten foil. Powder X-ray diffraction data were measured alternately with the EXAFS data using an X-ray wavelength of 1.4 Å, slightly lower in energy than the tungsten L_{III}-edge, for a period slightly less than 5 min over the range $2\theta \approx 11$–$72°$. Diffraction patterns were measured using an INEL curved, position-sensitive detector. The combined time for an EXAFS scan, collection of an XRD pattern and associated monochromator movement time was 10 min. Station 9.3 is equipped with a furnace which allows solid samples in the form of pellets to be heated to temperatures of 1000 °C. Three experiments were performed on ammonium tetrathiotungstate, all under an atmosphere of flowing dry nitrogen. In the first a sample was heated rapidly (20 °C min^{-1}) to 135 °C, below the lowest temperature reported for the onset of decomposition of the compound.[12] Then EXAFS and XRD data were collected with the temperature maintained at this level for 560 min. A second isothermal experiment was performed at 150 °C. In the third experiment a sample was heated rapidly to 100 °C at 20 °C min^{-1} then heated at 1 °C min^{-1} whilst measuring EXAFS and XRD data until the temperature had reached 350 °C. This is the temperature typically used to prepare the pc-WS_2 catalysts mentioned above.[10–13] Data were measured from crystalline 2H-WS_2 diluted in boron nitride at a variety of temperatures between room temperature and 500 °C to provide a direct comparison for the data collected from the decomposition products of ammonium tetrathiotungstate.

Data analysis

Calibration and background subtraction of the EXAFS data was performed using the programs EXCALIB and EXBACK and the data modelled in k-space with k^3-weighting from k = 3 to 16.3 $Å^{-1}$ using the program EXCURV92.[33] For each EXAFS spectrum the threshold energy was defined as the point of inflection of the near-edge region, and a post-edge

background calculated using a combination of three third-order polynomials. Phase-shifts were calculated within EXCURV92 using the Hedin–Lundqvist method for determining ground state potentials and exchange potentials calculated using the von Barth method. EXAFS spectra were Fourier transformed to produce a one-dimensional radial distribution function, using phase-shifts calculated for the first atomic shell.

Elemental analysis

The pellets used in the EXAFS/XRD experiment were retained after heat treatment and finely ground. X-Ray microanalysis was performed using a Philips CM20 transmission electron microscope fitted with an EDAX PV9900 detection unit and operating with an accelerating voltage of 200 keV. This allowed examination of particles containing only tungsten and sulfur without interference from the diluent boron nitride. The method of Cliff and Lorimer was used to perform elemental analysis.[34] A calibration constant was derived from study of the W-L and S-K emissions of crystalline 2H-WS_2 to convert the ratio of observed X-ray emission intensities to relative atomic concentrations. Typically ten metal sulfide particles in each mixture were analysed in this way.

Results

Isothermal decompositions

Fig. 2 shows powder diffraction patterns recorded during the heating of ammonium tetrathiotungstate at 135 °C. Bragg reflections of the crystalline starting material decrease in intensity as time proceeds. It can be seen that even after over nine hours of heating there is a small amount of ammonium tetrathiotungstate that has not decomposed. The Bragg reflections which have constant intensity throughout the experiment are due to the crystalline diluent boron nitride, and these have the same intensity at 560 min as at the beginning of the experiment indicating that decay of the incident beam was negligible over the period of heating. The ground pellet after heating contained a small amount of yellow material mixed with the grey tungsten sulfide product and the white boron nitride, consistent with the presence of some unreacted ammonium tetrathiotungstate, which is bright yellow. Elemental analysis of this mixture using the electron microscope showed the tungsten sulfide present to have composition $WS_{3.1(1)}$.

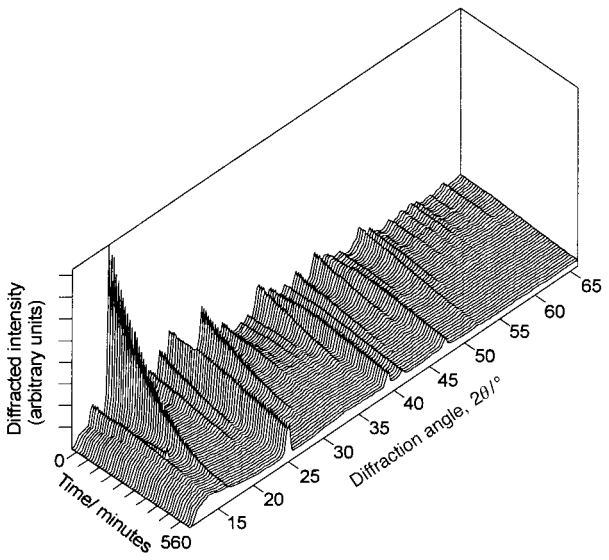

Fig. 2 X-Ray powder diffraction patterns recorded during the isothermal decomposition of ammonium tetrathiotungstate at 135 °C. Bragg peaks of constant intensity throughout the experiment are due to the crystalline diluent boron nitride.

The first EXAFS spectrum recorded during heating at 135 °C, Fig. 3(a), can be modelled as arising from a single shell of sulfur atoms at 2.19 Å. On varying all parameters describing this shell [occupation number (N), radial distance, (R) and Debye–Waller (A)] along with the threshold energy in least-squares refinements, convergence was achieved with the parameters shown in Table 1. The refined distance of 2.19 Å agrees well with the results of a previous crystallographic study of the ammonium tetrathiotungstate (2.17 Å)[35] and the refined coordination number of 3.80 is consistent with the tetrahedral environment of tungsten in the tetrathiotungstate anion, bearing in mind the large errors associated with EXAFS-derived coordination numbers. The data collected during 10–15 min of heating could similarly be modelled by a single shell, but on refinement of the structural parameters a lower coordination number resulted ($N_S = 3.68$). This is consistent with a small amount of ammonium tetrathiotungstate having decayed. The Fourier transform of the EXAFS data showed no evidence for any further atomic shells. The next 16 data sets could be modelled using the single shell model, but with a gradually decreasing first shell coordination number over time. Contour maps showing the effect of the pair of correlated parameters, N and A on the fit-index were calculated for each set of data, and showed that modelling the decreasing EXAFS amplitude with time as arising from a decrease in coordination number rather than an increase in static disorder (and hence Debye–Waller factor) was the best approach. The dramatic decrease of the amplitude of the EXAFS oscillations observed during decomposition produces a decrease in signal : noise ratio; this explains why the fit-index becomes higher during later scans.

To model the data measured between 160 and 165 min [Fig. 3(b)], two further shells of atoms were necessary, as indicated by a broad feature in the Fourier transform of the data beyond the first peak. A second shell of sulfur atoms at *ca.* 2.40 Å, and a shell of tungsten atoms at *ca.* 2.75 Å was found to give a satisfactory fit. The observation of a W–S shell and a W–W shell at the distances stated is indicative of the presence of a-WS_3; previous structural investigations of a-WS_3 prepared *ex situ* all find tungsten to have six to eight sulfur near neighbours at between 2.38 and 2.43 Å, and up to two W near neighbours at 2.60–2.80 Å.[23,24,36,37] The results of previous W L_{III}-edge EXAFS studies of a-WS_3 show that the sulfur shell has associated with it a large amount of static disorder, far greater than thermal disorder over a large range of temperature. In one study data collected at different temperatures between 80 K and ambient temperature showed the Debye–Waller factor of the sulfur shell to be independent of temperature within the errors of an EXAFS experiment.[37] In order to simplify modelling of the atomic shells due to a-WS_3 here, the Debye–Waller factors of the sulfur shell at 2.40 Å and of the tungsten shell at 2.75 Å were fixed at 0.03 and 0.01 $Å^2$ respectively, close to those previously determined by EXAFS. The validity of using these values at the higher temperature used here was tested later (*vide infra*). The EXAFS data have sufficient k-range to allow the remaining structural parameters describing all of the three shells to be refined in least-squares refinements (a total of eight independent parameters) and to allow the three shells to be resolved.‡ The results

‡The number of independent parameters, N_{ind}, that may be varied in EXAFS data analysis to give meaningful results is given by $N_{ind} \approx 2\Delta k \Delta R/\pi$, and the smallest separation of shells that can be resolved, Δr, by $\Delta r = \pi/2\Delta k$, where Δk is the extent of data in k-space, and ΔR the range of distance over which EXAFS data are being modelled (usually determined by inspection of the Fourier Transform).[38] For the data analysed here, $N_{ind} \approx 9$ and $\Delta r = 0.12$ Å, since $\Delta k = 13.3$ $Å^{-1}$ and taking ΔR to be 1 Å, since atomic shells between 2 and 3 Å are being considered.

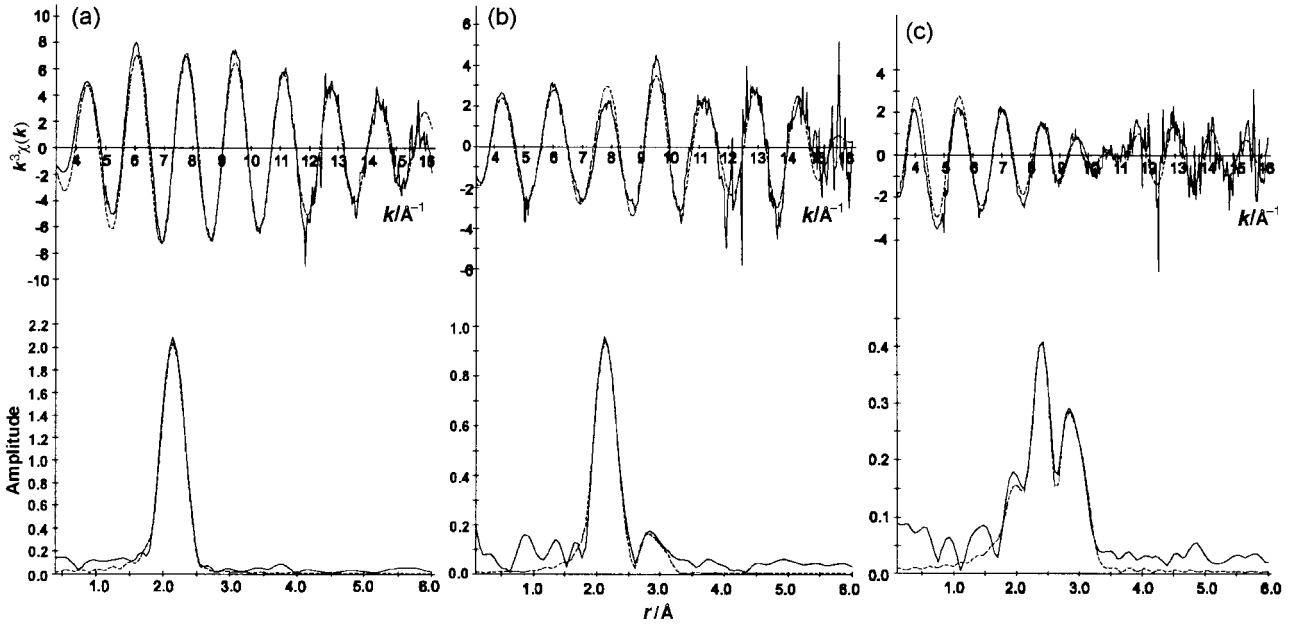

Fig. 3 Tungsten L_{III}-edge EXAFS spectra (k^3-weighted) and their Fourier transforms, recorded during the isothermal decomposition of ammonium tetrathiotungstate at 135 °C at (a) 0–5 min, (b) 160–165 min and (c) 560–565 min. Full lines are the experimental functions and broken lines those generated from models fitted to the data (see Table 1).

Table 1 Structural parameters determined by analysis of the tungsten L_{III}-edge EXAFS data collected during the thermal decomposition of ammonium tetrathiotungstate at 135 °C at selected times[a]

t/min	Shell	N	R/Å	A/Å^2	Fit index/10^{-4}
0–5	S	3.77(9)	2.193(1)	0.0050(2)	2.06
80–85	S	2.56(8)	2.189(1)	0.0043(3)	3.63
160–165	S	2.02(11)	2.167(3)	0.0042(5)	7.70
	S	1.42(31)	2.461(9)	0.03	
	W	0.81(1)	2.753(6)	0.01	
240–245	S	1.44(13)	2.161(4)	0.0052(9)	15.86
	S	2.52(34)	2.414(10)	0.03	
	W	1.08(10)	2.756(5)	0.01	
320–325	S	0.77(9)	2.155(4)	0.003(10)	15.67
	S	2.74(23)	2.370(9)	0.03	
	W	1.09(10)	2.748(4)	0.01	
400–405	S	0.61(11)	2.168(6)	0.0044(16)	14.54
	S	3.71(23)	2.385(9)	0.03	
	W	1.22(9)	2.75(4)	0.01	
480–485	S	0.39(10)	2.146(71)	0.0041(23)	12.41
	S	4.02(20)	2.364(81)	0.03	
	W	1.16(9)	2.751(35)	0.01	
560–565	S	0.21(8)	2.157(10)	0.0028(32)	11.93
	S	4.03(19)	2.375(8)	0.03	
	W	1.18(7)	2.757(4)	0.01	

[a] N is the shell occupation number, R its radial distance and A its Debye–Waller factor ($=2\sigma^2$); those without esds were fixed in least-squares refinements. Estimated errors are those resulting from least-squares refinements and take no account of experimental error. The fit-index is defined as $\sum_i (k^3(\chi_i^{calc}(k)-\chi_i^{exp}(k)))^2$, where χ_i^{calc} and χ_i^{exp} are the ith data point of the calculated and experimental X-ray absorption coefficient, respectively.

of fitting the three-shell model to the EXAFS data collected during 160–165 min are shown in Table 1. For later data sets, modelling was approached in exactly the same manner and the refined structural parameters showed a steady decrease in first shell coordination number with time, and a corresponding increase in second and third shell coordination numbers, reflecting the decay of the tetrathiotungstate anion and the growth of amorphous WS_3. Refined interatomic distances and the first shell Debye–Waller remained unchanged within experimental error (typically ± 0.02 Å for interatomic distances and $\pm 10\%$ for Debye–Waller factors). Refined parameters from data collected during selected times are shown in Table 1. After 560 min of heating the EXAFS data [Fig. 3(c)] show that there still remains a small amount of unreacted ammonium tetrathiotungstate, most clearly indicated by the Fourier transform which shows the short W–S shell is still necessary to model the data.

In the thermal decomposition of ammonium tetrathiotungstate at 135 °C we did not prepare pure a-WS_3 but nevertheless have gained new information about the system. Fig. 4(a) shows plots of the fractional change in area of the strongest ammonium tetrathiotungstate Bragg reflection (at 16.2°, deter-

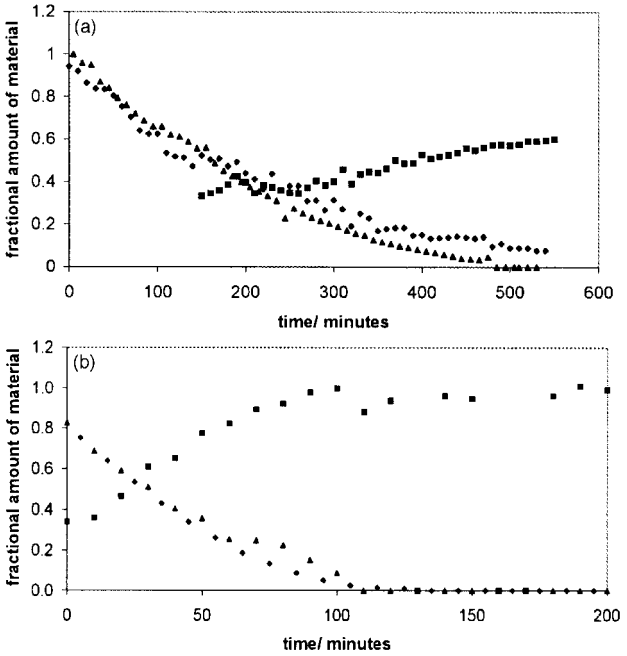

Fig. 4 Changes with time of the fractional occupation of the W–S shell at 2.19 Å necessary to model the EXAFS data (diamonds), the fractional area of the strongest Bragg reflection of ammonium tetrathiotungstate (triangles) and the fractional occupation of the W–S shell at 2.45 Å in the EXAFS data (squares) at (a) 135 °C and (b) 150 °C. See text for normalisation method.

mined by Gaussian fitting), the changing fractional occupation of the 2.17 Å sulfur shell (N_S) observed in the EXAFS data (normalised assuming $N_S=4$ at the beginning of the experiment), and the changing fractional occupation (N_W) of the 2.45 Å tungsten shell (normalised using $N_W=7$ at the end of the reaction when pure a-WS_3 is present, as we will show below). The two curves representing decay of ammonium tetrathiotungstate show excellent agreement, and the curve representing the formation of a-WS_3 intersects at ≈ 0.5. Both these results show that the approach to data analysis taken is a good model of the system, *i.e.* that ammonium tetrathiotungstate decomposes to form a-WS_3 without any intermediate of different local structure, so that each EXAFS spectrum can be modelled as a mixture of starting material and product during the process. It would appear from these data that at the beginning of the decomposition small amounts of a-WS_3 are difficult to detect in the presence of ammonium tetrathiotungstate by EXAFS. This is probably largely due to the high Debye–Waller factors associated with the atomic correlations in a-WS_3. One important point that has emerged here is that the large static disorder present in a-WS_3, responsible for the high Debye–Waller factor of the sulfur shell, severely limits the quality of EXAFS data that may be obtained from the compound. In this experiment with the same amount of absorbing element in the X-ray beam, the signal : noise ratio of the EXAFS data is dramatically reduced as ammonium tetrathiotungstate decomposes to produce a-WS_3.

A second isothermal experiment was performed at 150 °C with the aim of observing the formation of pure a-WS_3 in a reasonable time. Data analysis was approached in an identical manner to the first isothermal experiment. In this case thermal decomposition was much more rapid and the EXAFS data collected in the first 5 min of heating showed decomposition had already begun, since three shells (the same as in the previous experiment) were required to model the data, indicating the presence of a-WS_3. This was confirmed by the X-ray diffraction data, since the area of the strongest Bragg reflection had decreased compared to its intensity before heating. The X-ray diffraction data show that thermal decomposition was complete after 125 min of heating, and the EXAFS data collected just before this time (120–125 min) were the first to show no evidence for the short W–S distance characteristic of the tetrathiotungstate anion. Fig. 4(b) shows the decay curve of ammonium tetrathiotungstate and the growth curve of a-WS_3 at 150 °C derived in exactly the same manner as in the 135 °C experiment. As before, the EXAFS decay curve shows excellent agreement with that derived from XRD, and the growth curve of a-WS_3 intersects at ≈ 0.5, consistent with the two-phase approach taken to data analysis.

Both sets of isothermal data were used to investigate the kinetics of decomposition of ammonium tetrathiotungstate. The kinetics of reactions of the type A(solid)→ B(solid)+C(gas) under isothermal conditions have been widely studied in the past.[39] Thermal decompositions are complex processes which may exhibit up to five stages of reactions, each described by different kinetic expressions. A simple approach to analysing data from thermal decompositions is to assume that the 'acceleratory period', where physical changes are the largest with time and so most easy to detect, extends for the largest part of reaction. For the data measured here we use the X-ray diffraction decay curves to test three simple expressions commonly used to model thermal decomposition reactions; a simple exponential relationship, $\alpha=e^{k_1 t}$, the Avrami–Erofe'ev expression, $-\ln(1-\alpha)=(k_2 t)^n$ and the Prout–Tompkins expression, $\alpha/(1-\alpha)=e^{k_3 t}$. In each case α is the extent of reaction, scaled to zero at the beginning of the reaction and unity at the end, and k_n is a rate constant for the process. For the Avrami–Erofe'ev expression, n, the Avrami exponent, contains information about the mechanism of reaction. Fig. 5 shows three plots, which are expected to be

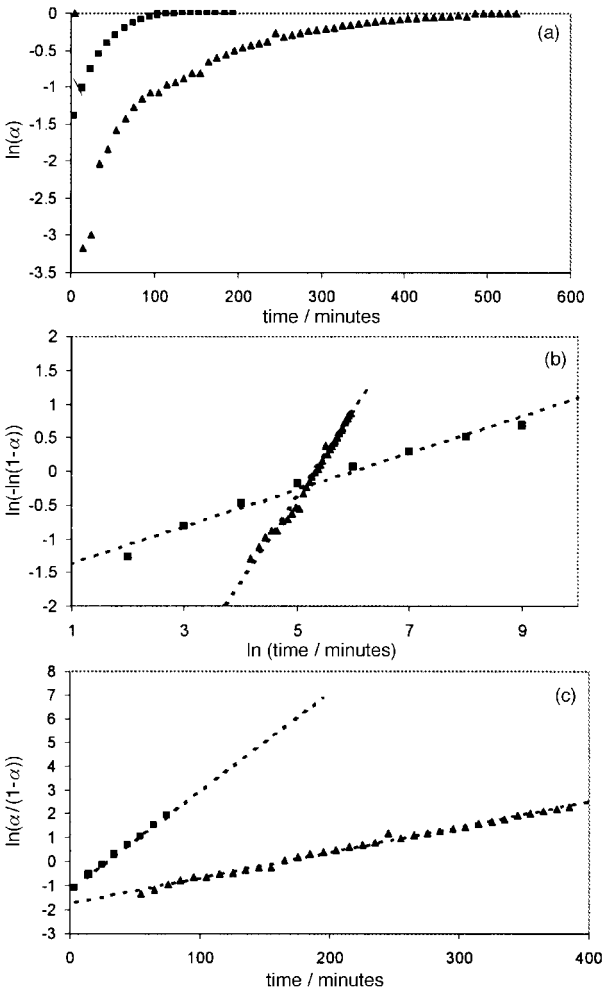

Fig. 5 Plots of (a) ln(α) *vs.* time, (*b*) ln(−ln(1−α)) *vs.* ln(time) and (c) ln(α/(1−α)) *vs.* time for 135 °C decomposition data (diamonds) and 150 °C data (squares) as tests for three kinetic models (see text). In (b) and (c) dotted lines are lines of best fit determined by linear regression.

linear if the expression tested holds, for values of α between 0.1 and 0.8. It can be seen the simple exponential model gives markedly non-linear plots for both temperatures studied. The Avrami–Erofe'ev expression gives reasonably linear graphs at each temperature but the very different gradient of each line (1.3 at 135 °C and 0.3 at 150 °C) would suggest that a different reaction mechanism operates at each temperature, which is unlikely and we have no other evidence for this being the case. The Prout–Tompkins model, Fig. 5(c), gives a much more sensible fit. For each temperature we can obtain a rate constant by determining the gradient using linear regression: 0.01 min^{-1} at 135 °C and 0.04 min^{-1} at 150 °C [best-fit lines are shown on Fig. 5(c)]. The differences in intercept must arise from the differences in induction time of the acceleratory period at each temperature, a quantity difficult to determine accurately, particularly with our simple approach to data analysis. The Prout–Tompkins expression was originally developed from a study of the thermal decomposition of potassium permanganate[40] and describes a mechanism involving the growth of chains of product material through the starting material, once nucleation sites have formed, which branch on encountering a grain boundary and terminate on mutual contact.[41]

At this point we consider the EXAFS data of freshly prepared a-WS_3, the decomposition product of ammonium tetrathiotungstate after 200 min heating at 150 °C, Fig. 6. Firstly as a check on the validity of fixing Debye–Waller factors of the two atomic shells of a-WS_3 during earlier data

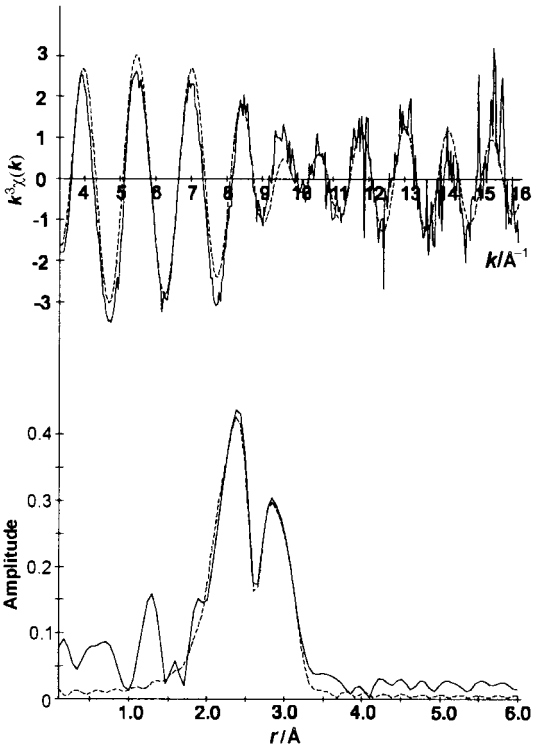

Fig. 6 Tungsten L_{III}-edge EXAFS spectrum (k^3-weighted) and its Fourier transform of a-WS_3 prepared *in situ* by thermal decomposition of ammonim tetrathiotungstate at 150 °C for 200 min.

analysis, all structural parameters were allowed to vary in least squares refinements (a total of seven independent parameters). The results confirm that the values used previously $A_S = 0.03$ Å^2 and $A_W = 0.01$ Å^2 were correct (see Table 2). The refined coordination numbers and interatomic distances are all consistent with previous studies of a-WS_3 prepared *ex situ*.[23,24,36,37] The refined W–W coordination number (N_W) of 1.6 does not provide conclusive evidence for either structural model for a-WS_3, *i.e.* those based on the W_2 dimer ($N_W = 1$), or those based on the W_3 triangular cluster ($N_W = 2$). One possible explanation is that both structure types are present. The large errors associated with coordination numbers derived from EXAFS and the difficulties in collecting high-quality data from the compound do not allow each model to be distinguished. An important point to consider is that our new data show no evidence for shells of radial distance greater than the tungsten shell at 2.75 Å; including extra sulfur or tungsten shells at distance of *ca.* 3 Å then performing least-squares refinements never produced a statistically significant improvement in fit. As indicated by Fig. 1, we might expect short non-bonded W···W distances (3–3.2 Å) in the chain model for a-WS_3, both along the inter- and intra-chain. The fact that EXAFS finds no evidence for such a distance suggests that if the chain structure comes close to portraying the true structure of a-WS_3 then there would be a large amount of static disorder associated with the non-bonded W···W correlations. Their contribution to the EXAFS signal would thus be very small. Other possibilities are that a-WS_3 contains W_3 triangular clusters or a mixture of both triangular and dimeric units. We hope to resolve the issue in future work by comparison with model compounds and by using diffraction methods, which give more reliable coordination numbers.

Table 2 Structural parameters determined by the tungsten L_{III}-edge study of a-WS_3 prepared *in situ* by heating ammonium tetrathiotungstate at 150 °C for 200 min. Legend as for Table 1

Shell	N	R/Å	A/ Å^2	Fit index/10^{-4}
S	6.98(41)	2.401(6)	0.0305(17)	6.48
W	1.56(24)	2.757(3)	0.0102(10)	

Decomposition under increasing temperature

In the third *in situ* experiment we heated ammonium tetrathiotungstate from 100 to 350 °C at 1 °C min^{-1} with the aim of preparing a sample of pc-WS_2 for detailed study. Fig. 7 shows the powder diffraction data collected during this experiment. In the initial stages of reaction the Bragg peaks of ammonium tetrathiotungstate decay to produce an amorphous phase (a-WS_3). The crystalline starting material has decayed completely when a temperature of 180 °C is reached and there are no sharp diffraction features (other than those due to the crystalline diluent) until a temperature of 315 °C is attained. At this point diffuse features appear at 2θ *ca.* 14, 30 and 53°. Fig. 8 shows the powder diffraction pattern collected between 345 and 350 °C. The broad diffraction features due to the decomposition product of ammonium tetrathiotungstate lie in the region of the 002, (100, 101, 102) and (110, 008) reflections of crystalline 2H-WS_2. The diffraction data presented here are very similar to those previously published for poorly crystalline WS_2.[14,16] The broad Bragg peaks and the change in their relative intensities are indicative of small crystallite size and stacking faults respectively; features that might be expected in WS_2 prepared at low temperature.

EXAFS data analysis for the data collected as ammonium tetrathiotungstate was heated from 100 to 350 °C was approached in exactly the same manner as describe above for the first two *in situ* experiments. Initially a single sulfur shell at 2.19 Å modelled the data well, until a temperature of 160 °C was reached when the two shells characteristic of a-WS_3 were necessary to provide a satisfactory fit (sulfur at *ca.* 2.40 Å and tungsten at *ca.* 2.72 Å). The data collected between 170 and 175 °C show no evidence for the short W–S distance of the tetrathiotungstate anion, and this is close to the temperature that the XRD data show the crystalline starting material to have decayed (175–180 °C). At this point pure a-WS_3 is present, and the structural parameters describing two atomic shells were included in least-squares refinements. The two-shell model fits the data recorded in the next nine scans very

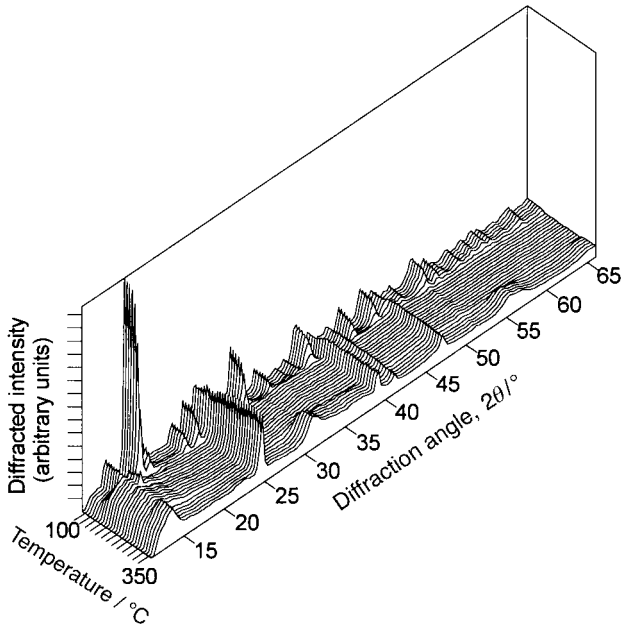

Fig. 7 X-Ray powder diffraction patterns recorded during the decomposition of ammonium tetrathiotungstate under a temperature gradient of 1 °C min^{-1}. Bragg peaks of constant intensity throughout the experiment are due to the crystalline diluent boron nitride.

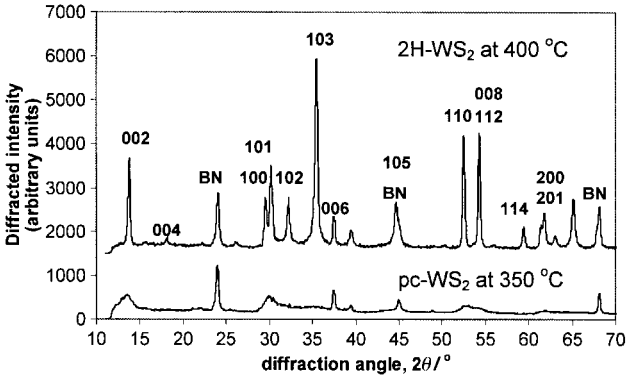

Fig. 8 X-Ray powder diffraction patterns of pc-WS_2 (prepared *in situ* at 350 °C) and 2H-WS_2. Miller indices of the strongest Bragg reflections of 2H-WS_2 are shown and those of the crystalline diluent boron nitride are indicated by BN.

well, and all structural parameters were allowed to vary for these data sets. This produced values matching those determined above for a-WS_3; coordination numbers of 5–7 and 1–1.5 and Debye–Waller factors of *ca.* 0.03 and 0.01 Å^2 for the sulfur and tungsten shells, respectively. The results of data analysis from selected scans are shown in Table 3. The data collected between 310 and 315 °C were the first to show any further change. This temperature is just before the XRD data indicate the formation of poorly crystalline WS_2. The EXAFS data also indicate the presence of WS_2 by a characteristic non-bonded W···W distance at 3.15 Å, which is seen in 2H-WS_2[41] [see Table 3 and Fig. 9(a)]. It should be noted that in common crystalline forms of WS_2 tungsten is surrounded by six equidistant sulfur atoms at 2.41 Å so little change in first shell is expected during the transformation of a-WS_3 to WS_2. However the short W–W bond (2.75 Å) of a-WS_3 provides a means of tracking the decay of the amorphous sulfide and it was found that this process is rapid under the conditions we used. Data collected between 330 and 335 °C contain no indication of the short W–W distance of a-WS_3 and the refined occupation number of the W···W shell at 3.15 Å has increased to $\approx$4. The data collected at 350–355 °C [Table 3 and Fig. 9(b)] show little further change and it is these that we consider to investigate the structure of poorly crystalline WS_2.

EXAFS data collected from crystalline 2H-WS_2 at 400 °C, shown in Fig. 9(c), can be compared with those collected from poorly crystalline WS_2. The Fourier transform shows two distinct atomic shells as well as broad features at higher radial distance. Clearly the sharp peaks can be assigned as the nearest sulfur shell (2.41 Å) and tungsten shell (3.15 Å) and the results of varying all structural parameters of these two shells in least-squares refinements are shown in Table 4. The refined coordination numbers are reasonably close to those expected (both six), and the fit-index is little affected if these are fixed at the crystallographic values, and other parameters refined. A significant improvement in fit results if a third shell (of sulfur atoms) is added to the structural model; this accounts for the broad features beyond the 3.15 Å peak of the EXAFS Fourier transform, and corresponds to a non-bonded interlayer atomic correlation.[41] Coordination numbers were all fixed at crystallographic values to reduce the number of structural parameters varied in refinement. It can be seen that the refined atomic distances show excellent agreement with those determined crystallographically (Table 1). The third shell was found to be statistically significant at the 1% probability level on application of the Joyner test.[42] The fit of exactly the same structural models was tested for the EXAFS data from pc-WS_2 prepared *in situ* at 350 °C, Table 3. It can be seen that modelling the data with coordination numbers fixed at the expected values for the two atomic shells gives a considerably worse fit than if the coordination numbers of both shells are reduced. If the coordination of the first shell is fixed at six and the other varied in least–squares refinement along with all other parameters, the fit obtained is significantly worse than the model with both coordination numbers reduced. The data from pc-WS_2 are best modelled if a third atomic shell of sulfur atoms is included in the model. The average radial distances of these three shells are essentially identical to those observed in 2H-WS_2, immediately suggesting the structure of the poorly crystalline WS_2 is closely related to the crystalline forms of WS_2 in which tungsten is surrounded by a trigonal prism of six sulfurs. The EXAFS Fourier transform [Fig. 9(b)] of pc-WS_2 compared to that of 2H-WS_2 shows that the magnitude of all peaks is considerably reduced in intensity. Although least-squares refinements of all parameters of the first two atomic shells suggest that low coordination number is responsible for this, because of the high correlation between coordination numbers and Debye–Waller factors it is difficult to determine whether this is truly the case. Unfortunately, the presence of the third atomic shell precludes the detailed analysis of the correlations between N and A for the first two shells, which we were able to carry out for pc-MoS_2.[21] Chemical and physical considerations would suggest that the most reasonable explanation is that for the first sulfur shell the coordination number is six and that there is appreciable static disorder associated with this shell.

These first EXAFS data measured from pc-WS_2 must be compared to those previously determined for pc-MoS_2 prepared similarly. Nanocrystalline MoS_2 has been extensively studied by EXAFS at the Mo K-edge, because of its great importance in hydrodesulfurisation processes, and it is now widely accepted that MoS_2 prepared by the thermal decomposition of ammonium tetrathiomolybdate is structurally simi-

Table 3 EXAFS-derived structural parameters determined during the heating of ammonium tetrathiotungstate under a temperature gradient (1 °C min^{-1}) at selected temperatures. For key see Table 1

T/°C	Shell	N	R/Å	A/Å^2	Fit-index/10^{-4}	Interpretation
100–105	S	3.78(8)	2.193(1)	0.0048(2)	1.97	$(NH_4)_2WS_4$
150–155	S	3.07(10)	2.189(2)	0.0055(3)	2.57	$(NH_4)_2WS_4$ + a-WS_3
	S	1.13(24)	2.516(19)	0.03		
	W	0.35(8)	2.763(10)	0.01		
200–205	S	4.67(15)	2.390(6)	0.03	9.48	a-WS_3
	W	0.90(7)	2.750(3)	0.01		
250–255	S	4.60(30)	2.388(6)	0.0311(18)	7.94	a-WS_3
	W	1.05(11)	2.741(3)	0.0104(11)		
310–315	S	3.11(8)	2.399(4)	0.03	8.66	a-WS_3 + pc-WS_2
	W	0.22(2)	2.736(4)	0.01		
	W	1.61(43)	3.144(7)	0.0173(3)		
350–355	S	3.67(13)	2.403(2)	0.0201(7)	4.44	pc-WS_2
	W	2.97(39)	3.158(3)	0.0098(5)		

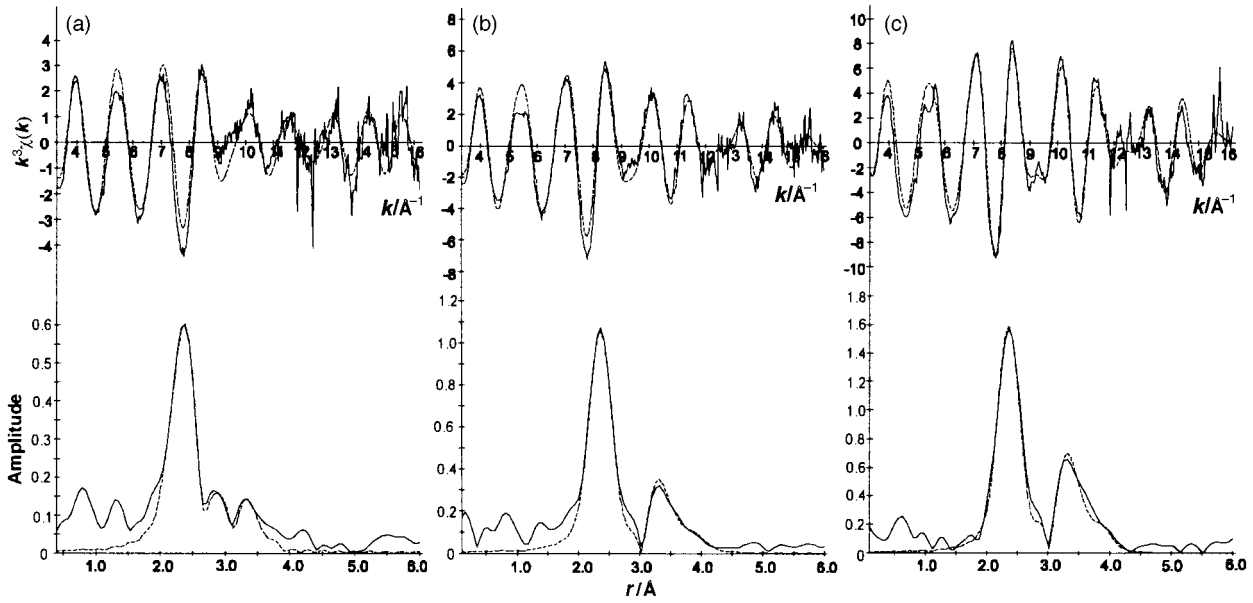

Fig. 9 Tungsten L_{III}-edge EXAFS spectra (k^3-weighted) and their Fourier transforms, recorded during the thermal decomposition of ammonium tetrathiotungstate under increasing temperature; (a) at 310–315 °C (mixture of a-WS_3 and pc-WS_2), (b) 350–355 °C (pc-WS_2) and (c) of 2H-WS_2 at 400 °C. Full lines are the experimental functions and broken lines those generated from models fitted to the data (see Tables 3 and 4 for structural parameters).

Table 4 Structural models fitted to the tungsten L_{III}-edge EXAFS data of 2H-WS_2 at 400 °C and pc-WS_2 prepared *in situ* at 350 °C. Crystallographic parameters for 2H-WS_2 are also shown for comparison. See Table 1 for key.

Compound	Model	Shell	N	R/Å	A/Å^2	Fit-index/10^{-4}
2H-WS_2	Crystal	S	6	2.405	—	
at 400 °C	structure	W	6	3.153	—	
	(ref. 41)	W	6	3.966	—	
	A	S	6	2.400(2)	0.0107(3)	4.40
		W	6	3.164(3)	0.0147(4)	
	B	S	5.08(18)	2.402(2)	0.0088(5)	4.14
		W	6.83(63)	3.165(3)	0.0156(8)	
	C	S	6	2.399(2)	0.0107(3)	4.01
		W	6	3.161(2)	0.0148(4)	
		S	6	3.957(11)	0.0232(3)	
pc-WS_2	A	S	6	2.405(3)	0.0169(4)	7.59
at 350 °C		W	6	3.158(4)	0.0201(7)	
	B	S	3.67(13)	2.403(2)	0.0098(5)	4.44
		W	2.97(39)	3.158(3)	0.0144(1)	
	C	S	4	2.403(2)	0.0108(3)	4.52
		W	3	3.157(3)	0.0144(5)	
	D	S	6	2.403(3)	0.0163(4)	7.41
		W	2.43(43)	3.156(4)	0.0127(12)	
	E	S	4	2.402(2)	0.0107(3)	4.25
		W	3	3.157(3)	0.0145(5)	
		S	2.72(1.16)	3.956(16)	0.040(9)	

lar. Two very recent publications provide useful summaries of the literature relating to pc-MoS_2.[43,44] Calais *et al.* highlight the discrepancy between particle size of nanocrystalline MoS_2 determined by EXAFS and electron microscopy when a conventional structural model is used to interpret the EXAFS data based on small slabs of 2H-MoS_2 whose edges are bounded by sulfur atoms.[43] Shido and Prins reconcile this problem by proposing a new model in which distortions at the particle edges mean that Mo···Mo distances are up to 0.16 Å greater than in 2H-MoS_2, and edges are not exclusively bounded by sulfur atoms.[44] In our recent study of pc-MoS_2 prepared *in situ* we reached the conclusion that not only small particle size was responsible for the low crystallinity of the compound, but that static disorder from the ideal 2H-MoS_2 structure must also contribute to the disorder,[21] consistent with the model of Shido and Prins. In all EXAFS studies of pc-MoS_2 disorder is associated with the second (Mo) shell of molybdenum and the first (S) shell is essentially the same as in 2H-MoS_2. The data we present here show that pc-WS_2 differs considerably from pc-MoS_2 in that the first coordination shell of tungsten, as well as further ones, is disordered compared to 2H-WS_2, and that a third atomic shell is clearly visible. It is curious that notwithstanding the higher degree of disorder in the first two shells of pc-WS_2, a third atomic shell is clearly visible. This contrast with the situation for pc-MoS_2 in which all molybdenum K-edge EXAFS studies reveal only the first two shells. The great difficulty in separating the contribution of various types of disorder from three atomic shells make it difficult to reach a firm conclusion and produce a structural model for the disorder in pc-WS_2. It is possible that some of the disorder in the first coordination shell is a relic of the high disorder in the sulfur shell in a-WS_3 which is not observed in a-MoS_3, the precursor of pc-MoS_2.

Conclusions

In this *in situ* study we have been able to monitor the thermal decay of a crystalline precursor to form an amorphous product, and ultimately a poorly crystalline solid. The changes in intensity of the EXAFS signal during the process highlight the great difficulty in collecting high quality data from a-WS_3. Nevertheless we have extracted kinetic data and been able to model the process using an expression wholly appropriate for a thermal decomposition reaction. It must be remembered that the kinetics of thermal decompositions are extremely sensitive to a large number of experimental factors, such as sample particle size, sample volume, method of sample preparation (sample history), heating rate applied and even the physical change being detected, and so the results obtained here should perhaps not be compared too closely with those that may be determined using other techniques. It is especially important to bear in mind that when using X-rays as structural probes thermal decomposition may be enhanced because of sample fracture and thus an increase in grain boundaries.[45]

The formation of poorly crystalline WS_2 *in situ* by continued heating of a-WS_3 has allowed the first EXAFS data to be collected from this catalytically active material. We have shown that the material differs structurally from its molybdenum counterpart, and suggested means of describing the disorder of the compound. Clearly the material is worthy of a more detailed structural study, for example by analysis of diffuse X-ray scattering, which would require diffraction data of much greater quality than we have obtained in the current work, or by electron microscopy. This is a line of future research we will pursue.

Acknowledgement

We thank the EPSRC for a studentship (R.I.W.) and for provision of facilities at Daresbury Laboratory. We are grateful to Dr A.J. Dent of Daresbury Laboratory for his assistance with running the EXAFS/XRD experiment.

References

1 R. Prins, V. H. J. De Beer and G. A. Somorjai, *Catal. Rev.—Sci. Eng.*, 1989, **31**, 1.
2 T. Weber, J. C. Muijsers, J. H. M. C. van Wolpot, C. P. J. Verhagen and J. W. Niemantsverdriet, *J. Phys. Chem.*, 1996, **100**, 14144.
3 B. K. Miremadi, K. Colbow and S. R. Morrison, *J. Appl. Phys.*, 1997, **82**, 2639 and references therein.
4 A. J. Jacobson, R. R. Chianelli, S. M. Rich and M. S. Whittingham, *Mater. Res. Bull.*, 1979, **14**, 1437.
5 J. J. Auborn, Y. L. Barberio, K. J. Hanson, D. M. Schleich and M. J. Martin, *J. Electrochem. Soc.*, 1987, **134**, 581.
6 K. Ramanathan and S. W. Weller, *J. Catal.*, 1985, **95**, 249.
7 S. P. A. Louwers and R. Prins, *Jpn. J. Appl. Phys.*, 1993, **32**, 457.
8 M. Remsikar, Z. Skraba, M. Regula, C. Ballif, R. Sanjines and F. Levey, *Adv. Mater.*, 1998, **10**, 246.
9 R. Tenne, M. Homyonfer and Y. Feldman, *Chem. Mater.*, 1998, **10**, 3225.
10 T. Osaki, H. Taoda, T. Horiuchi and H. Yamakita, *React. Kinet. Catal. Lett.*, 1993, **51**, 39.
11 J. Ramírez, P. Castillo, A. Benitez, A. Vasquez, D. Acosta and A. Lopéz-Agado, *J. Catal.*, 1995, **158**, 181.
12 K. Wilkinson, M. D. Merchán and P. T. Vasudevan, *J. Catal.*, 1997, **171**, 325.
13 G. Alonso, M. Del Valle, J. Cruz, A. Licea-Claverie, V. Petranovskii and S. Fuentes, *Catal. Lett.*, 1998, **52**, 55.
14 R. J. H. Voorhoeve and H. B. M. Wolters, *Z. Anorg. Allg. Chem.*, 1970, **376**, 165.
15 T. P. Prasad, E. Diemann and A. Müller, *J. Inorg. Nucl. Chem.*, 1973, **35**, 1895.
16 J. C. Wildervanck and F. Jellinek, *Z. Anorg. Allg. Chem.*, 1964, **328**, 309.
17 R. R. Chianelli, *Int. Rev. Phys. Chem.*, 1982, **2**, 127.
18 D. A. Rice, S. J. Hibble, M. J. Almond, K. A. Hassan Mohammad and S. P. Pearse, *J. Mater. Chem.*, 1992, **2**, 895.
19 S. J. Hibble, D. A. Rice, M. J. Almond, K. A. Hassan Mohammad, S. P. Pearse and J. R. Sagar, *J. Mater. Chem.*, 1992, **2**, 1237.
20 S. J. Hibble, R. I. Walton, D. M. Pickup and A. C. Hannon, *J. Non-Cryst. Solids*, 1998, **232–234**, 434.
21 R. I. Walton, A. J. Dent and S. J. Hibble, *Chem. Mater.*, 1998, **11**, 3737.
22 K. S. Liang, J. P de Neufville, A. J. Jacobson and R. R. Chianelli, *J. Non-Cryst. Solids*, 1980, **35**, 1249.
23 K. S. Liang, S. P. Cramer, D. C. Johnston, C. H. Chang, A. J. Jacobson, J. P de Neufville and R. R. Chianelli, *J. Non-Cryst. Solids*, 1980, **42**, 345.
24 S. P. Cramer, K. S. Liang, A. J. Jacobson, C. H. Chang and R. R. Chianelli, *Inorg. Chem.*, 1984, **23**, 1215.
25 A. Müller, E. Diemann, E. Krickemeyer, H-J. Walberg, H. Bögge and A. Armatage, *Eur. J. Solid State Inorg. Chem.*, 1993, **30**, 565.
26 Th. Weber, J. C. Muijsers and J. W. Niemantsverdriet, *J. Phys. Chem.*, 1995, **99**, 9194.
27 E. Diemann, *Z. Anorg. Allg. Chem.*, 1977, **432**, 127.
28 J. W. Couves, J. M. Thomas, D. Waller, R. H Jones, A. J. Dent and G. N. Greaves, *Nature*, 1991, **345**, 465.
29 S. R. Davis, A. V. Chadwick and J. D. Wright, *J. Phys. Chem. B*, 1997, **101**, 9901.
30 M. Epple, G. Sankar and J. M. Thomas, *Chem. Mater.*, 1997, **9**, 3127.
31 I. J. Shannon, T. Maschmeyer, G. Sankar, J. M. Thomas, R. D. Oldroyd, M. Sheehy, D. Madill, A. D. Waller and R. P. Townsend, *Catal. Lett.*, 1997, **23**, 23.
32 B. S. Clausen, *Catal. Today*, 1998, **39**, 293.
33 N. Binstead, J. W. Campbell, S. J. Gurman and P. C. Stephenson, *EXCURV92*, SERC Daresbury Laboratory, 1991.
34 G. Cliff and W. Lorimer, *J. Microsc.*, 1975, **105**, 205.
35 K. Sasvari, *Acta Crystallogr.*, 1963, **16**, 719.
36 R. R. Scott, A. J. Jacobson, R. R. Chianelli, W-H. Pan, E. I. Stiefel, K. O. Hodgson and S. P. Cramer, *Inorg. Chem.*, 1986, **25**, 1461.
37 S. J. Hibble, D. A. Rice, D. M. Pickup and M. P. Beer, *J. Chem. Soc., Faraday Trans.*, 1996, **92**, 2131.
38 *Report on the International Workshops on Standards and Criteria in XAFS* in *X-ray Absorption Fine Strucure*, ed. S. S. Hasnain, Ellis Horwood, Chichester, 1991, p. 751.
39 F. C. Tompkins, *Decomposition Reactions in Treatise on Solid State Chemistry*, ed. N. B. Hannay, Plenum Press, New York, 1976, vol. 4, ch. 4. p. 193.
40 E. G. Prout and F. C. Tompkins, *Trans. Faraday Soc.*, 1944, **40**, 488.
41 W. J. Schutte, J. L. de Boer and F. Jellinek, *J. Solid State Chem.*, 1987, **70**, 207.
42 R. W. Joyner, K. J. Martin and P. Meehan, *J. Phys. C: Solid State Phys.*, 1987, **20,** 4005.
43 C. Calais, N. Matsubayashi, C. Geantet, Y. Yoshimura, H. Shimada, A. Nishijima, M. Lacroix and M. Breysse, *J. Catal.*, 1998, **174**, 130.
44 T. Shido and R. Prins, *J. Phys. Chem. B*, 1998, **102**, 8426.
45 C. N. R. Rao and J. Gopalakrishan, *New Directions in Solid State Chemistry*, Cambridge University Press, Cambridge, 1997, p. 481.

Paper 9/00956F